Building and Environment 168 (2020) 106499

Contents lists available at ScienceDirect

Building and Environment

journal homepage: http://www.elsevier.com/locate/buildenv

VOC emissions from nail salon products and their effective removal using affordable adsorbents and synthetic jets

A. Lamplugh [a], M. Harries [b], A. Nguyen [c], L.D. Montoya [c,*]

[a] Department of Mechanical Engineering, 1111 Engineering Drive, UCB 427, University of Colorado Boulder, Boulder, CO, 80309-0427, USA
[b] Department of Physics, 2000 Colorado Avenue, UCB 390, University of Colorado Boulder, Boulder, CO, 80309-0390, USA
[c] Department of Civil, Environmental, and Architectural Engineering, 1111 Engineering Drive, UCB 428, University of Colorado Boulder, Boulder, CO, 80309-0428, USA

ARTICLE INFO

Keywords:
Adsorption
Coco coir
Biochar
Passive removal
Active flow
Cosmetics

ABSTRACT

Volatile organic compounds (VOCs) like acetone, ethyl and n-butyl acetate, toluene, and formaldehyde have been measured inside nail salons, where they are emitted from nail care products. Exposure to these compounds can have negative health impacts on both workers and costumers, as well as the environment. The objectives of this research were to characterize VOC emissions from typical nail care products and to investigate VOC removal by 3 low-cost adsorbent materials (coco coir, biochar, and activated carbon). The removal studies were performed using acetone as the model VOC in both chamber experiments and mathematical models. The chamber experiments were conducted under both passive and active flow conditions using synthetic jet actuators to determine the effect of local ventilation on the rate of removal. Mass-normalized adsorption rates were determined for acetone using nth-order rate equations. Adsorption rate models were then developed for all adsorbent materials under both flow conditions and used to estimate the effect of low-cost adsorbents in an actual nail salon. Activated carbon provided the best VOC removal compared to the other 2 adsorbent materials tested. The use of active flow with synthetic jets was also shown to enhance adsorption processes for both biochar and activated carbon, but not for coco coir. Model results predicted activated carbon with active flow enhancement could achieve an effective ventilation rate of nearly 300 $m^3 h^{-1}$ if 250 kg were placed in a 1400 m^3 salon.

1. Introduction

Americans work an average of 34.5 h per week [1] and spend close to 90% of their time indoors [2]. Consequently, much of their exposure to airborne pollutants occurs indoors, including occupational environments. Volatile organic compounds (VOCs) are air pollutants ubiquitous in the indoor environment, and hundreds of them have been measured inside non-industrial buildings [3]. VOCs have also been found in workplaces, where industrial operations and solvent use can release them into the air [4]. Previous studies in nail salons identified VOCs like acetone, toluene, ethyl acetate, methyl methacrylate, and formaldehyde [5–7], which are emitted from nail products [8,9]. Exposure to these compounds is known to cause skin, eye, and respiratory irritation as well as headaches, neurological issues [10], reproductive complications [11], and cancer [12].

Mitigating occupational exposures to indoor air pollution has traditionally been accomplished by increasing the ventilation rate of a building. Ventilation problems in nail salons have been documented, including non-functioning [13] and undersized [14] ventilation systems. While some states and municipalities have adopted ventilation standards that apply to nail salons, including the International Mechanical Code [15], many of these rules only apply to new salons and include vague language that provides limited guidance [16]. Pavilonis [17] investigated VOC levels at salons in the state of New York, which has specific ventilation requirements for new and existing nail salons, and found that CO_2 levels correlated strongly with VOC concentrations. Furthermore, when CO_2 levels exceeded target concentrations set by the American National Standards Institute/American Society of Heating, Refrigerating and Air-Conditioning Engineers (ANSI/ASHRAE), a nearly tenfold increase in VOC levels was observed.

Many VOCs commonly found in the indoor environment could be removed from the air through adsorption. The adsorption process involves gas-phase molecules (adsorbates) bonding to the solid surface of a material (adsorbent) through physical or chemical processes [18]. In contrast to chemical adsorption, physical adsorption processes are reversible, and adsorbents can be regenerated thermally [19]. In the

* Corresponding author.
E-mail address: lupita.montoya@colorado.edu (L.D. Montoya).

https://doi.org/10.1016/j.buildenv.2019.106499
Received 30 May 2019; Received in revised form 17 September 2019; Accepted 23 October 2019
Available online 24 October 2019

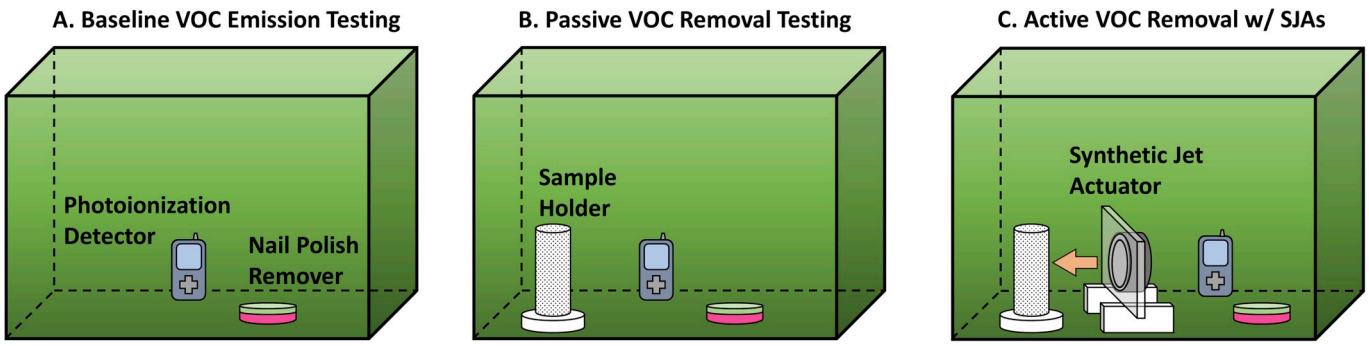

Fig. 1. Experiments performed to evaluate adsorbent materials in a controlled environment: A) baseline emissions from nail care product, B) passive VOC removal and C) active VOC removal using a synthetic jet actuator.

indoor environment, adsorbent materials have been shown to act as VOC sinks, reducing concentrations of indoor pollutants when ventilation rates are insufficient [20]. In some cases, natural and engineered sorbent materials have been used to create passive, diffusion-based VOC removal systems for the built environment, which can improve indoor air quality [21,22].

Alternative, sustainable adsorbents like biochar [23,24] and char-based activated carbon from agricultural feedstocks [25] have received some attention in recent years as potential VOC adsorbents. Raw, natural adsorbent materials like coconut husk (coco coir) [26,27] and rice husk [28] have also been investigated, primarily for water-quality applications. Despite the popularity of these adsorbent materials, and claims that they may be more environmentally friendly than traditional adsorbents [23], relatively little is known about their adsorption potential, especially with regard to VOC removal.

Among factors that influence adsorption processes are near-surface fluid conditions [29], which can be controlled and optimized. Synthetic jet actuators (SJAs) are low-cost, energy efficient devices used to generate jet flows and have been shown to affect the direction of air flows in a room [30] and to enhance the removal of pollutants from indoor air [31,32]. One recent study [33] also found that vortex rings from synthetic jets can penetrate through porous surfaces, and even form downstream transmitted vortex rings.

The goal of this study was to quantify VOC emissions from common nail care products and assess the capability of 3 affordable adsorbents to remove emissions of acetone, as a model VOC, using controlled experiments and mathematical models. In this study, the total VOC content from a common nail polish remover was determined using gravimetric and headspace analyses. The VOC emissions from this product were also determined in a closed environmental chamber. VOC removal using coco coir, biochar, and activated carbon as adsorbent materials was investigated in this closed chamber under both passive and active flow conditions using SJAs. VOC removal rate models were then developed for these 3 adsorbents under both flow conditions. The resulting models were applied to time-resolved VOC concentration data from a previous field study to estimate the impact these materials could have on air quality inside an actual nail salon.

2. Materials

2.1. Nail care products

Five nail care products (3 nail polishes and 2 nail polish removers) were used in this study and are listed in Supplementary Information Table S1, along with product information provided in the manufacturer safety data sheet (SDS). All products were obtained from retail stores or nail salons in the Denver-Boulder, CO area. A single acetone-based nail polish remover (product PR-2) was then used in the VOC removal experiments and modeling exercises. All nail care products used were obtained new, in sealed containers, and were stored in a temperature-controlled environment throughout the duration of the study. All VOC removal experiments described here were performed with nail polish remover from the same bottle.

2.2. Adsorbent materials

A total of 3 different absorbent materials were tested in this study: coco coir (CC), biochar (BC), and activated carbon (AC). Each material was tested in two sizes: fine (<355 μm) and coarse (355–841 μm) grains. CC was purchased from Sunleaves Garden Products (Mooresville, IN), BC was obtained from Biochar Solutions (Carbondale, CO), and MICROBE-LIFT® AC pellets were purchased from Ecological Laboratories, Inc. (Malverne, NY).

2.3. Environmental test chamber

All non-gravimetric experiments in this study were performed inside a sealed environmental chamber made of 316 stainless-steel with dimensions 75 cm (W) x 75 cm (H) x 121 cm (L) (0.68 m^3 total volume). A leak test was performed on the chamber using carbon dioxide (CO_2) as the tracer gas. CO_2 concentrations in the chamber were measured with an Extech SD800 CO_2 datalogger (Extech, Nashua, NH, Range: 0–4000 ppm, Accuracy: ±5%, Resolution: 1 ppm). CO_2 concentrations outside of the chamber were measured with a Telaire T7001 CO_2 monitor (Onset Computer Corporation, Bourne, MA, Range: 0–2500 ppm, Accuracy: ± 50 ppm) connected to an Onset Hobo U12-013 Temp/RH/2 external channel logger (Onset, Bourne, MA, Temp Range: 20 °C – 70 °C, Temp Accuracy: ±0.35 °C, RH Range: 5%–95%, RH Accuracy: ±2.5%).

Ultra-pure 99.999% CO_2 (Airgas, Cinnaminson, NJ) was introduced into the chamber until the concentration was approximately 3900 ppm, after which the monitor was allowed to equilibrate for 8 h. CO_2 concentrations were then recorded for 66.5 additional hours in 5 s intervals. The average external CO_2 concentration was 448 ppm (±25 ppm). The average leakage (exchange) rate for the chamber was determined to be 1.7×10^{-5} m^3 h^{-1}, or 2.5×10^{-5} air changes per hour. Temperature and relative humidity (RH) in the chamber were fairly constant for all experiments performed; temperature ranged from 20.4 °C to 22.6 °C with a mean of 21.1 ± 0.002 °C, and RH ranged from 21.0% to 39.1% with a mean of 27.9 ± 0.02%.

3. Methods

3.1. Material preparation and characterization

The adsorbent materials were first ground using a Nasco-Asplin soil grinder (Patent #2,903,198, NASCO, Fort Atkinson, WI) and then sized using U.S.A standard test sieves #20 and #45. Surface area (SA), pore size, and volume, were determined for all materials using Brunauer-Emmett-Teller (BET) and Barrett-Joyner-Halenda (BJH) analyses. Prior

to analysis, samples were degassed overnight at 100 °C and <50 mTorr. Analyses were performed on a Micromeritics Gemini V 2380 surface area analyzer (Micromeritics Instrument Corp., Norcross, GA). Each sample underwent a 5-point BET analysis, as well as a 40-point BJH desorption analysis. The BET surface area (BET SA), Langmuir SA, BET pore width, BJH pore width, and pore volume of each material were measured.

3.2. Experimental setup

Fig. 1 shows the 3 sets of experiments performed in the chamber. First, a series of experiments were used to determine the baseline VOC emissions from nail care products (Fig. 1A) using a photoionization detector (PID). Next, the experiment was repeated in the presence of adsorbent materials contained in a cylindrical sample holder (Fig. 1B) to determine the passive VOC removal by each adsorbent material. Finally, the VOC removal experiment was repeated with active flow provided by a SJA, which was directed at the adsorbent material (Fig. 1C).

In all 3 experiments, the concentrations of Total Volatile Organic Compounds (TVOCs) were measured using a HalTech HVX-501 Photoionization Detector (Hal Technologies, Fontana, CA, Range 0–200 ppm, Resolution 0.03 ppm) with a 3-min sampling frequency. The PID was calibrated for acetone at two points (0 ppm and 175 ppm) using a zero-air standard (Scott Specialty Gases, Plumsteadville, PA, O_2: 20–21%, Total Hydrocarbon: < 1 ppm) and an acetone gas standard (GASCO, Oldsmar, FL, Acetone: 175 ppm), respectively. The line between these points was used to determine the PID correction factor for acetone (1.56). Temperature and relative humidity (RH) in the chamber were measured with an Onset Hobo U12-013 Temp/RH/2 External Channel Logger (Onset, Bourne, MA, Temp Range: 20 °C – 70 °C, Temp Accuracy: ±0.35 °C, RH Range: 5%–95%, RH Accuracy: ±2.5%).

3.3. Headspace analysis

Headspace analysis was conducted on the nail polish remover (PR-2), using gas chromatography coupled with mass spectrometry (GC-MS), to determine the composition of gas-phase emissions from the product. Seven compounds in total were included in the calibration standards: ethyl acetate, n-butyl acetate, propyl acetate (n-propyl and isopropyl isomers quantified together), ethanol, isopropanol (2-propyl alcohol), acetone, and methyl acetate.

Samples were prepared by placing approximately 0.5 mL of PR-2 in a 4 mL septum-capped vial, which was allowed to equilibrate at room temperature for at least 1 h. The initial masses of PR-2 used in each sample were measured using an Ohaus Analytical Plus AP250D balance (Ohaus, Florham Park, NJ). Using a 10 μL gas-tight syringe primed 3 times with headspace vapor, a sample consisting of 5 μL headspace and a 1 μL plug of air was manually introduced to the GC-MS. The syringe was cleaned between injections and tested with regular blanks. Reported results are the average of 3 injections per sample (n = 3). The reproducibility of manual injections was tested with replicate injections of pure acetone. Two standard solutions were prepared in cyclohexanone to quantify all 7 compounds. One stock solution contained ethyl acetate, n-butyl acetate, propyl acetate (n-propyl and isopropyl isomers quantified together), ethanol, and isopropanol (2-propyl alcohol), while the other contained acetone and methyl acetate. Separate standards were prepared due to the co-elution of acetone and isopropanol. Serial dilutions of the standards were used to create a calibration curve for each compound across the range of concentrations expected in the samples. Triplicate injections were averaged to generate each curve.

3.4. Baseline VOC emissions from nail products

The density and total VOC content of PR-2 were determined using a simple gravimetric analysis. Briefly, 3 samples of PR-2 (0.1 mL) were placed into pre-weighed auto-sampling vials. Their masses were then measured using a TR-64 balance (Denver Instrument, Bohemia, NY, Max: 61 g, Precision: 0.1 mg). Samples were placed in a fume hood, uncovered, and allowed to evaporate over 10 h. The mass of PR-2 remaining in the vials was then measured again. The VOC content (mg g^{-1}) was reported as the average mass difference between pre and post-emission measurements (n = 3), divided by the average mass of product used. Additional gravimetric analyses were performed for PR-2 at volumes of 0.2 and 0.3 mL. Theoretical equilibrium concentrations ($C_{eq,theo}$) of acetone from PR-2, were calculated using the VOC content from the gravimetric analysis (mg) and dividing it by the volume of the closed chamber (m^3). These values were then compared with the equilibrium concentrations measured with the PID ($C_{eq,PID}$) to determine experimental deviation from predicted values.

Baseline emission testing was performed inside the closed chamber as shown in Fig. 1A. In each experiment, a standard volume of 0.1, 0.2, or 0.3 mL of PR-2 was used. Initial volumes of PR-2 are referred to here as low concentration (LC), medium concentration (MC), or high concentration (HC) for 0.1 mL, 0.2 mL, or 0.3 mL, respectively. PR-2 was measured using a 2 mL glass pipette and then placed in a glass Petri dish inside of the environmental chamber, which was promptly sealed. The PR-2 was then allowed to evaporate for 22.5 h. Before the chamber was sealed for each experiment, the internal pressure was equilibrated with the external pressure of the laboratory. Baseline VOC emission testing was performed 3 times (n = 3). Similar experiments were conducted for NP-1, NP-2, NP-3, and PR-1 using 1.0 mL of product. TVOC concentration curves were generated along with standard error values, and emission profiles were then plotted and compared.

3.5. Passive VOC removal with raw adsorbent materials

In these experiments, 20 g of CC, BC, or AC were used as the adsorbent. The individual materials were loaded into a custom-made, 3D printed sample holder (Fig. 1B), made of poly-lactic acid (PLA) with dimensions: height 12.5 cm, diameter 3 cm, wall thickness 0.25 cm. The sample holder was covered on the outside with two layers of 100% nylon mesh material. The mesh prevented the adsorbent material from escaping during the experiment but was permeable to gases in the chamber. The loaded sample holder was placed near the center of the chamber, the nail polish remover was added, and then the chamber was sealed.

Each VOC removal experiment was performed 3 times (n = 3) with the LC volume (0.1 mL) of PR-2. This experiment was also performed once (n = 1) with both MC (0.2 mL) and HC (0.3 mL) volumes of PR-2.

3.6. Active VOC removal using synthetic jet actuators

In the active flow experiments (Fig. 1C), VOC removal was achieved using raw adsorbent materials and enhanced using active flow provided by a ZFlow 87 Synthetic Jet Actuator (SJA) (Aavid Thermalloy, Laconia, NH, 5VDC, 95 mA, 475 mW). See Appendix A in the Supplementary Information for additional details about this SJA. A similar model of SJA from the same manufacturer was previously characterized [34] and used in a proof of concept experiment [31]. In the active flow experiments, the SJA was directed at the sample holder from a distance of 30 cm and operated throughout the duration of the experiment. Active VOC removal experiments were performed once at LC, MC, and HC using fine grain CC, BC, and AC.

3.7. Data analysis

Concentrations of acetone (PR-2) from baseline and (passive and active flow) removal experiments were first converted from ppm to mass-based concentrations, using the equation:

$$C_{mass}\left[mg\ m^{-3}\right] = C_{ppm} \times CF \times MW/(RT/P) \quad [1]$$

Table 1
Results from BET and BJH analyses.

Sorbent	Size[a]	BET SA (m^2 g^{-1})	Langmuir SA (m^2 g^{-1})	BET Pore Width (Å)	BJH Pore Diameter (Å)	BJH Pore Volume[b] (cm^3 g^{-1})
AC	Fine	916.7	1231	–	30.50	0.2059
	Coarse	957.4	1297	20.70	28.74	0.2158
BC	Fine	5.893	8.001	37.71	131.0	0.0041
	Coarse	5.030	6.791	27.78	114.6	0.0009
CC	Fine	5.759	7.963	83.66	171.2	0.0173
	Coarse	4.035	4.458	99.63	166.7	0.0114

[a] Fine (<355 μm); Coarse (355–841 μm).
[b] Desorption cumulative volume of pores between 17 and 3000 Å.

where P is the surface pressure in Boulder, CO (0.803 atm), R is the universal gas constant (0.08206 L atm mol^{-1} K^{-1}), T is the mean chamber temperature (K) during the experiment, MW is the molecular weight of acetone, and CF is the acetone correction factor for the PID (1.56).

To reduce noise in the VOC removal time series, concentration data were binned in intervals of approximately 15 min and presented as the geometric mean of that range. Since BET and BJH surface areas were reported per unit mass (m^2 g^{-1}), acetone removal was normalized by the mass of adsorbent used in the chamber. It was assumed that the loosely-packed adsorbent in the sample holder allowed for adsorption site access throughout the mass of the adsorbent sample. The normalized mass of acetone removed at each point in time, q(t) (mg g^{-1}), was calculated as:

$$q(t) = \frac{V_{chamber}}{m_{sorb}}[C_o(t) - C(t)] \quad [2]$$

where $V_{chamber}$ is the volume of the environmental chamber (0.68 m^3), $C_o(t)$ is the baseline concentration at t (mg m^{-3}), C(t) is the concentration at t during the removal test (mg m^{-3}), and m_{sorb} is the mass of adsorbent material in the chamber (g).

The adsorption rate of each material was then calculated over 22.5 h using the equation:

$$k_{ads,exp}(t) = \frac{q(t + 0.5\Delta t) - q(t - 0.5\Delta t)}{\Delta t} \quad [3]$$

where $k_{ads,exp}$ is the experimental VOC adsorption rate at time (t), which is the midpoint between two data points, and Δt is the time between the two data points (approximately 15 min).

Adsorption rate data for all 3 materials at the 3 VOC concentration levels, and 2 flow conditions, were fitted using R (v3.2.5) non-linear least squares regression analysis. Results were used to develop VOC adsorption rate models for each material of the form:

$$k_{ads} \sim f\{C(t), q(t)\} \quad [4]$$

3.8. Model of VOC removal for nail salons

A simple box (mass balance) model was developed in R (v3.2.5) to predict the impact of using adsorbent materials to reduce VOC concentrations inside a nail salon. This model was then applied under both active and passive flow conditions. Time-resolved TVOC data from a previous nail salon field study [5] were used as model inputs, and new VOC concentrations (C_{new}) were calculated using the adsorption rate

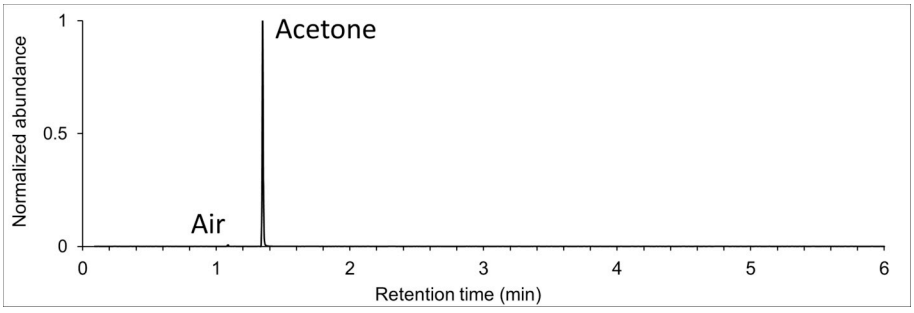

Fig. 2. TIC Chromatogram from acetone-based nail polish remover (PR-2) headspace analysis.

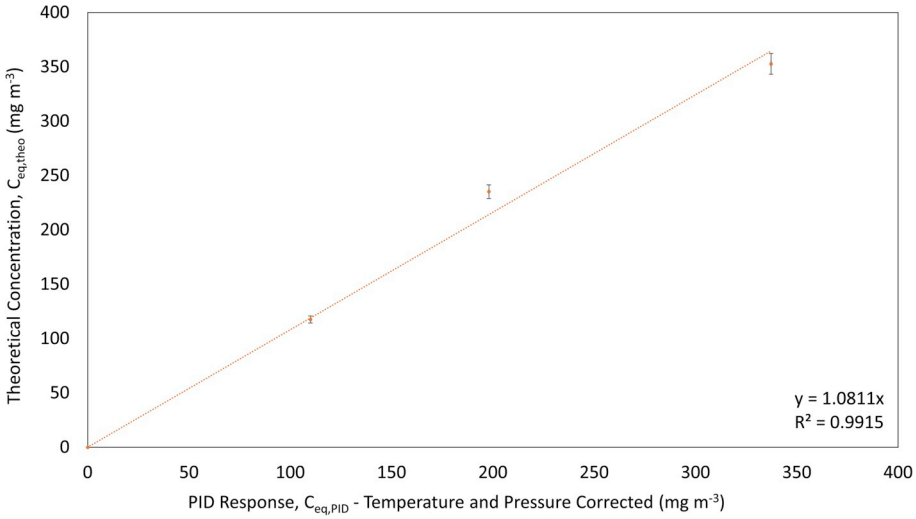

Fig. 3. Theoretical equilibrium acetone concentrations compared to measured concentrations from baseline emission tests.

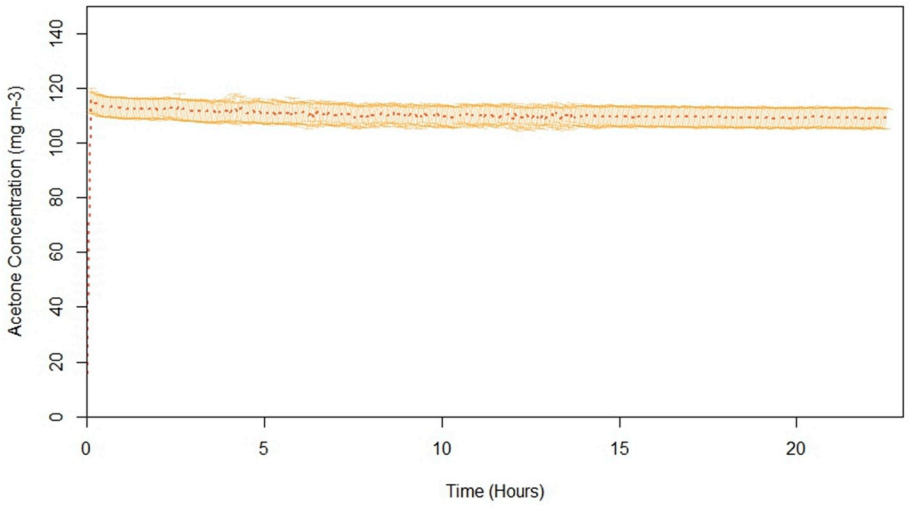

Fig. 4. Baseline acetone emission profile from PR-2 over 22.5 h with standard error bars.

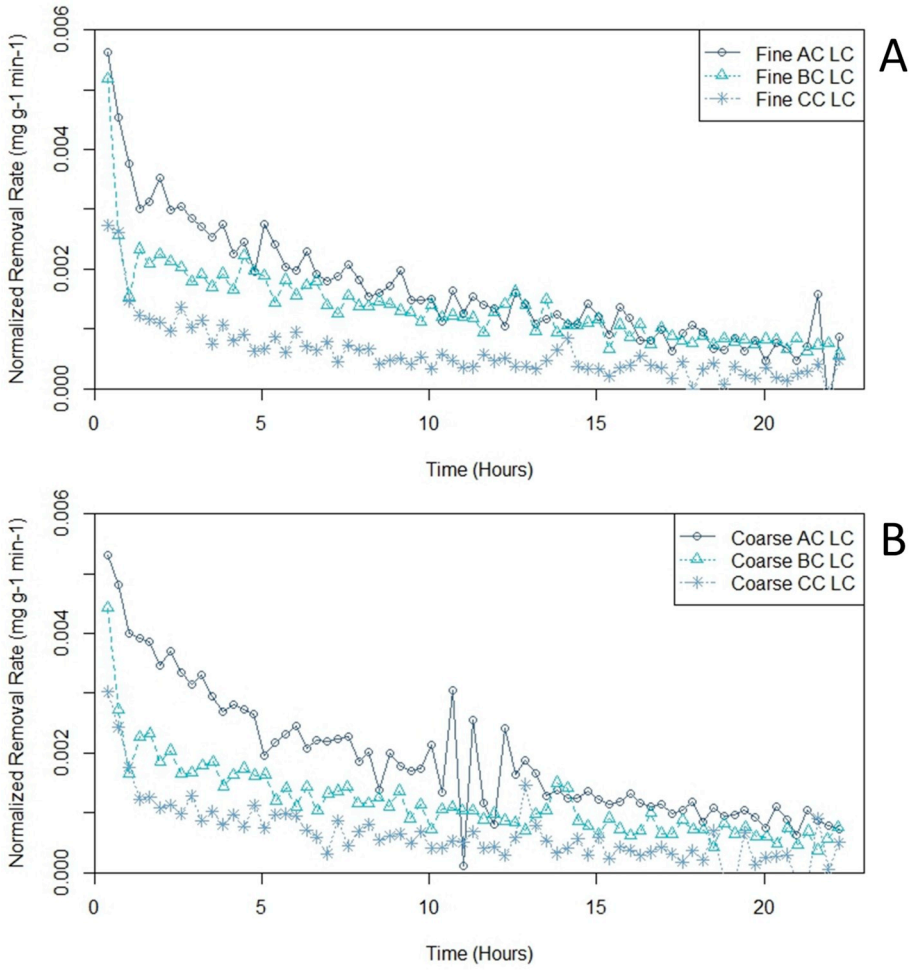

Fig. 5. Passive adsorption rates for (A) fine and (B) coarse CC, BC, and AC at LC across 22.5 h.

models determined for each material, from Eq. (4).

For purposes of this exercise, the field TVOC concentrations (measured with a PID) were assumed to be acetone. The correction factor for acetone (1.56) was applied to convert ppm to mass concentrations. Eq. (5) shows the mass balance performed at each time-step:

$$C_{new,i} = C_{field,i} + \frac{[\dot{m}_{i-1} \times (t_i - t_{i-1}) + k_{ads,i-1} \times m_{sorb} \times (t_i - t_{i-1})]}{V_{salon}} \quad [5]$$

where i is the time-step, t is time (min), V_{salon} is the volume of the salon (m^3), $C_{field,i}$ is the VOC concentration (mg m^{-3}) measured during the field study at i, m_{sorb} is the mass of the adsorbent used (g), and $\dot{m}$ is the

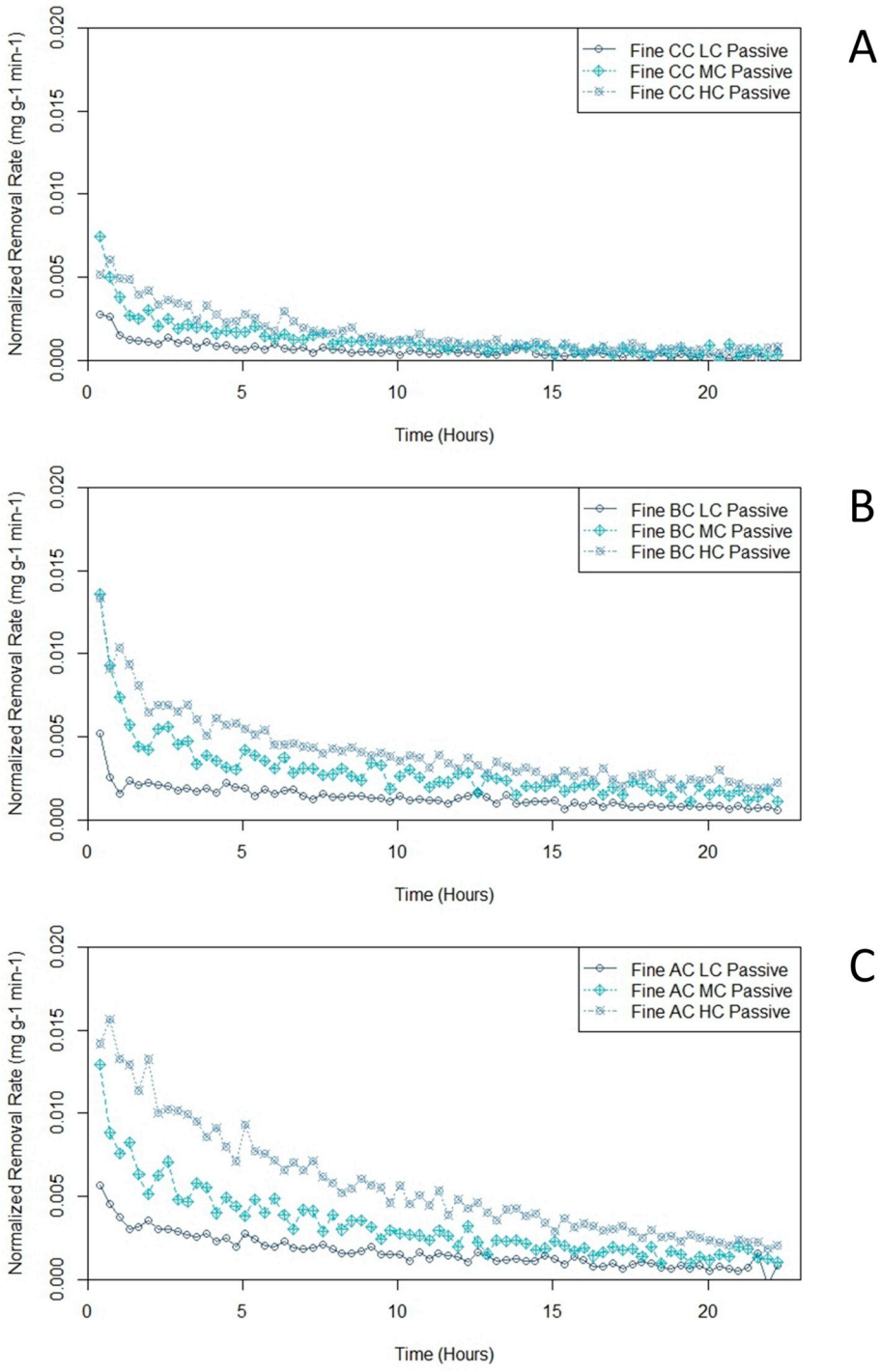

Fig. 6. Passive adsorption rates for fine (A) CC, (B) BC, and (C) AC at LC, MC, and HC across 22.5 h.

derivative of VOC mass with respect to time (mg min^{-1}) calculated from field study concentration data:

$$\dot{m}_i = \frac{V_{salon}\left[C_{field,i+1} - C_{field,i-1}\right]}{t_{i+1} - t_{i-1}} \quad [6]$$

This term accounted for changes in the mass of acetone in the salon air due to all processes (e.g., ventilation, chemical reactions, and emission) except adsorption onto the test materials. This step was necessary since the impact of each of these other processes could not be determined independently.

The total predicted mass of VOCs adsorbed over the 8 h period was reported along with an average effective ventilation rate (Q_{eff}), which was calculated as:

$$Q_{eff}\left(\frac{m^3}{hr}\right) = \frac{q_{total} \times m_{sorb}}{8h \times C_{med}} \quad [7]$$

where q_{total} is the predicted total mass of VOCs adsorbed per gram of adsorbent (mg g^{-1}), over the 8 h removal period and C_{med} is the median concentration (mg m^{-3}) of VOCs during the same time period.

Q_{eff} was used to estimate the contribution of the adsorbents toward indoor air-cleaning operations and allowed comparisons with traditional ventilation rates. A similar metric was previously employed by

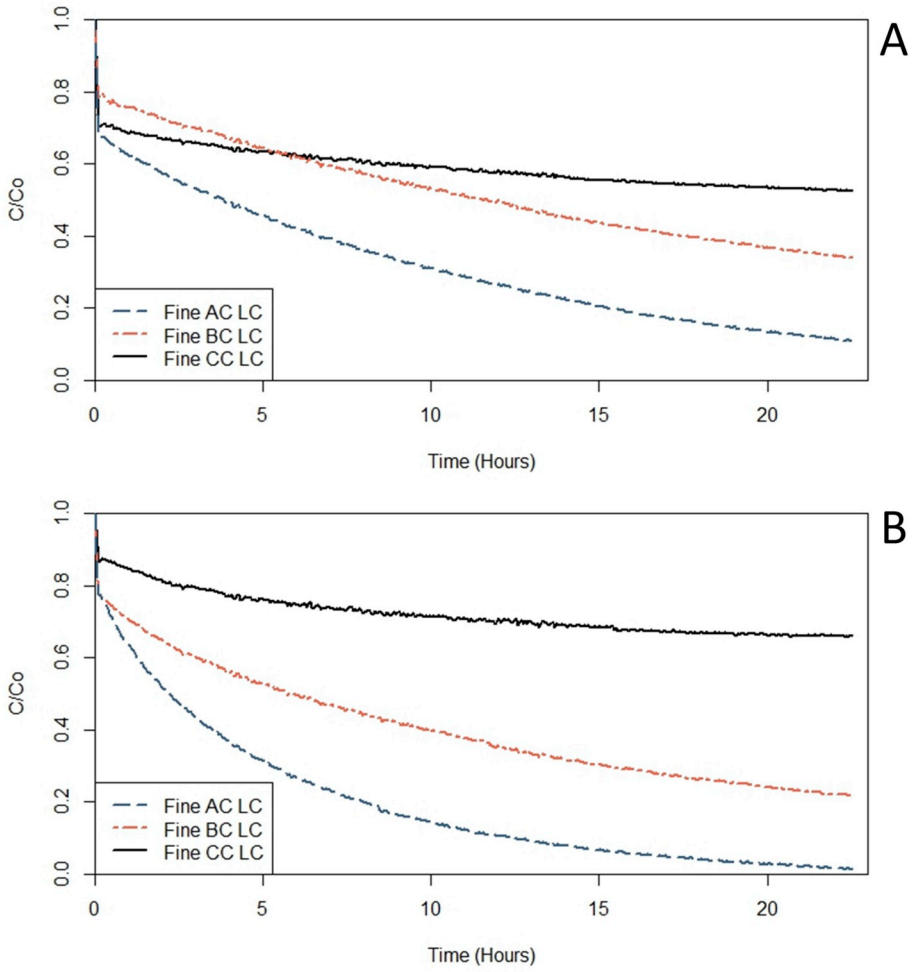

Fig. 7. Acetone removal using AC, BC, and CC at LC over 22.5 h under (A) passive flow, and (B) active flow provided by a SJA at 30 cm from the adsorbent material.

Ataka [35] and Huang [21]. The effective ventilation rate estimated in this study does not account for other non-VOC air pollutants that may be present indoors, including particulate matter and CO_2, and approximates a constant ventilation rate across all 8 h from a clean source of air (i.e., with no acetone). A volume-normalized metric was also considered, which is referred to here as the effective air exchange rate (ACH_{eff}), and was calculated as:

$$ACH_{eff} = \frac{Q_{eff}}{V_{salon}} \quad [8]$$

where V_{salon} is the volume of the nail salon (m^3) and ACH_{eff} is in hr^{-1}.

4. Results

4.1. Materials characterization

Results from the materials characterization, using BET and BJH analyses, are shown in Table 1. The analyses determined that AC had the greatest surface area and pore volume of all three materials characterized, followed by BC and CC. The particle size of the material (i.e. fine or coarse) had relatively little impact on the SA, except in the case of CC, where fine particles had a 43–79% greater SA than the coarse material. The pore volume of BC and CC were affected by particle size: fine BC had 356% more pore volume than coarse BC and fine CC had 52% more pore volume than coarse CC. The average pore width (BET) and average pore diameter (BJH) of both fine and coarse AC were substantially smaller (2–3 nm) than those of all BC or CC types. This pore size range fell at the intersection of what the International Union of Pure and Applied Chemistry (IUPAC) defines as microporous (<2 nm) and mesoporous (2–50 nm) [36]. Both BC and CC fell well within the range of mesoporous materials. Distributions of pore surface area and pore volume showed that a significant portion of BC and CC pore volume is located in macroporous structures (>50 nm).

4.2. Headspace analysis

Results from the headspace analysis showed that the only VOC emitted by PR-2 was acetone. A total ion count (TIC) chromatogram from the headspace analysis is shown in Fig. 2.

4.3. Baseline VOC emissions from nail products

Gravimetric analysis of PR-2 found a density of 0.799 ± 0.013 and VOC content of 1000 ± 41 ($mg\,g^{-1}$). Results from the gravimetric analysis were then compared to $C_{eq,PID}$ for acetone to determine if predicted values matched experimental PID measurements. Fig. 3 shows $C_{eq,theo}$ versus $C_{eq,PID}$ for PR-2 at LC, MC, and HC. The resulting 1:1 line has a slope of 1.0811 and an R^2 of 0.9915, indicating that measured concentrations of acetone closely matched theoretical predictions (within 9%), based on gravimetric results. This demonstrates that VOC loss from leakage, surface deposition, and emission prior to chamber sealing was minimal.

Fig. 4 shows the baseline VOC emission profile for PR-2. Fig. S1in the Supplementary Information shows emission profiles for the 5 nail care products included in this study. Results show that acetone emissions

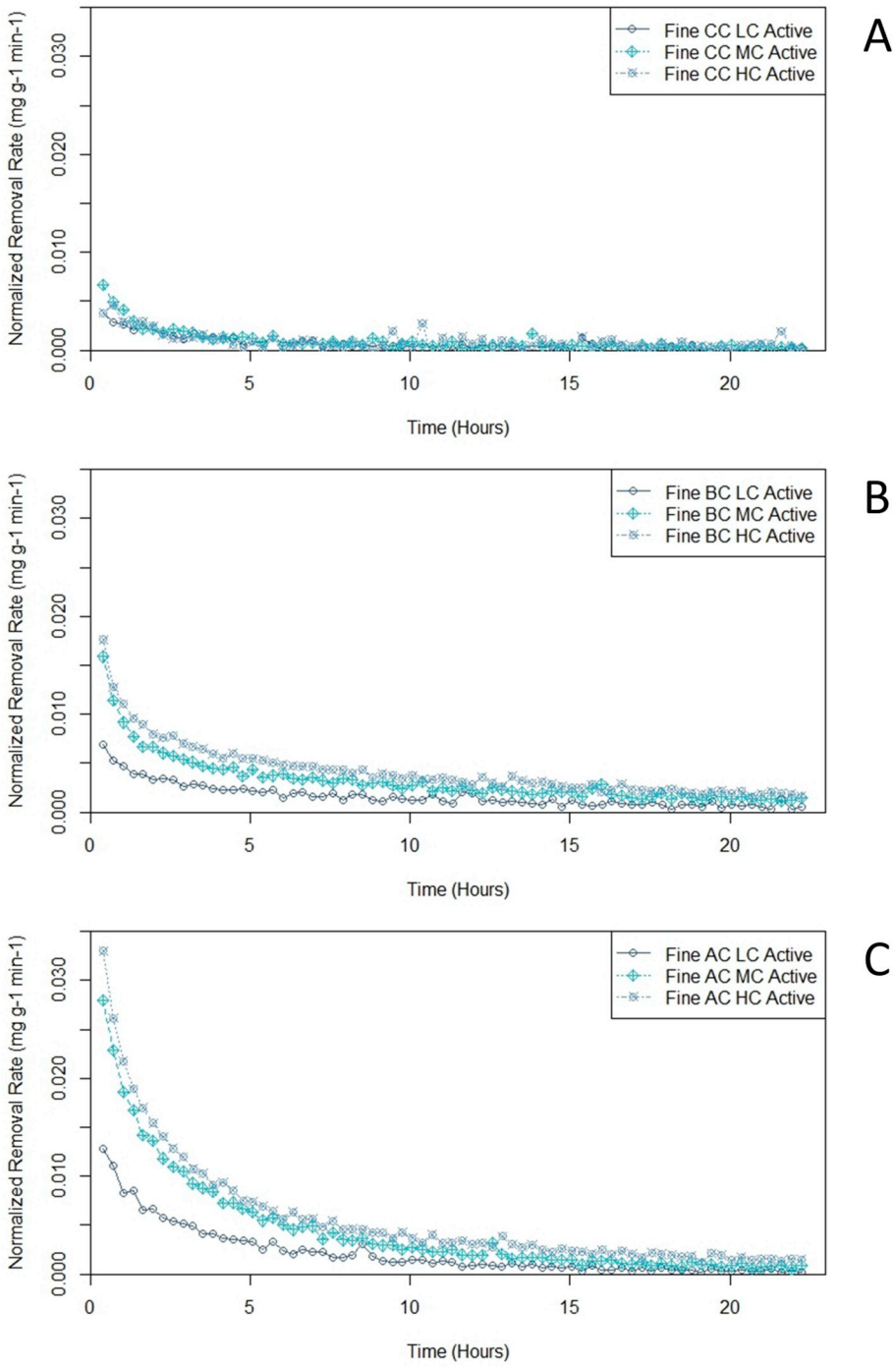

Fig. 8. Normalized adsorption rates for fine (A) CC, (B) BC, and (C) AC at LC, MC, and HC under active flow conditions.

from PR-2 reached equilibrium in approximately 40 min.

4.4. Passive VOC removal with raw adsorbent materials

PR-2 removal rates from passive adsorption experiments with fine and coarse CC, BC, and AC at LC from PR-2 are shown in Fig. 5A and B, respectively. Of all 3 fine grain materials, AC showed the highest adsorption rates during most of the 22.5 h test period (0.0056–0.0009 mg g^{-1} min^{-1}), followed closely by BC (0.0052–0.0006 mg g^{-1} min^{-1}) and CC (0.0027–0.0005 mg g^{-1} min^{-1}). Coarse grain materials followed a very similar trend, with AC performing the best (0.0053–0.0007 mg g^{-1} min^{-1}), followed by BC (0.0044–0.0008 mg g^{-1} min^{-1}) and CC (0.0030–0.0005 mg g^{-1} min^{-1}). These results suggest that the size distribution of adsorbent particles has little impact in passive adsorption rates. They also agree with the BET and BJH analyses, which showed that fine and coarse particles of each material had very similar properties overall.

Passive removal rates for all materials decreased by 50% or more during the initial 5 h. After 20 h, all materials showed removal rates near zero (<0.001 mg g^{-1} min^{-1}), although none of the materials reached equilibrium. Coarse AC removal data showed significant variability between 10 and 14 h (Fig. 5B). A review of the data suggests that this was likely due to a temporary sensor malfunction during one of the 3 removal experiments used in calculating the average rate values.

Fig. 6A, B, and C show adsorption rates of fine CC, BC, and AC at different concentrations of VOCs (LC, MC, and HC, respectively) emitted

Table 2
VOC mass removed and effective ventilation rates from adsorption models.

Passive Flow		Total VOC Removed (g)	Q_{eff} ($m^3\ h^{-1}$)	ACH_{eff} (h^{-1})
Fine CC	10 kg	7.09	16.7	0.01
	50 kg	29.9	70.5	0.05
	250 kg	76.4	179	0.13
Fine BC	10 kg	7.75	18.2	0.01
	50 kg	31.8	74.9	0.05
	250 kg	77.4	182	0.13
Fine AC	10 kg	12.4	29.3	0.02
	50 kg	45.1	106	0.08
	250 kg	94.4	222	0.16
Active Flow		**Total VOC Removed (g)**	**Q_{eff} ($m^3\ h^{-1}$)**	**ACH_{eff} (h^{-1})**
Fine CC	10 kg	2.46	5.79	0.00
	50 kg	11.6	27.2	0.02
	250 kg	43.2	101	0.07
Fine BC	10 kg	10.8	25.6	0.02
	50 kg	41.3	97.3	0.07
	250 kg	90.3	213	0.15
Fine AC	10 kg	24.1	56.8	0.04
	50 kg	68.1	160	0.11
	250 kg	124	292	0.21

from PR-2. The rate of adsorption was found to increase significantly with increased VOC concentration, and scaled approximately linearly with respect to the initial concentration of VOC (acetone). It was also observed that higher concentrations lead to greater total mass of VOCs adsorbed by each material, as previously reported in the literature [37,38]. The passive adsorption rates for all fine grain materials (CC, BC, AC) at MC and HC concentrations are included in Supplementary Fig. S2. The best-fit model for adsorption rates measured in this study was a nth-order equation similar to the one proposed by Ritchie [39]:

$$k_{ads} = a^{*}C(t)\left(1 - \frac{q(t)}{1.05^{*}q_{max}}\right)^{n} \quad [9]$$

where C(t) is the concentration of VOCs at a given time, q(t) is the normalized mass of VOCs adsorbed (mg g^{-1}) at the same time, a is a rate constant for each material, n is an exponent related to the order of the reaction (number of gas molecules adsorbed per adsorption site), and q_{max} (mg g^{-1}) is a quasi-equilibrium value of the maximum mass adsorbed onto 1 g of the material observed at HC and t = 22.5 h. Since q_{max} is only a quasi-equilibrium value, a factor of 1.05 was applied to approximate the actual equilibrium value. Similar nth-order models have previously been proposed for bio-adsorbents [40], and can account for unknown adsorption mechanisms as well as materials with heterogeneous surfaces. Supplementary Table S2 includes fitting values and correlations for each material under passive and active flow conditions for the model based on Eq. (9). Fitted removal rate graphs for all cases considered are shown in Supplementary Fig. S3.

4.5. Active VOC removal using synthetic jet actuators

Results from the VOC removal experiments using fine CC, BC, and AC at LC are shown in Fig. 7. Concentrations (C) from these removal experiments were normalized by their corresponding baseline VOC concentrations (C_0) and plotted as C/C_o. Fig. 7A shows the case for passive flow; Fig. 7B shows the case for active flow case, which was provided by a SJAs at a distance of 30 cm from the adsorbent material. Results show that AC was the most effective adsorbent; CC was the least effective. None of the adsorbents reached equilibrium within the 22.5 h testing period; an initial fast removal was also observed for CC and BC. The effect of the SJAs is noticeable when compared to the passive adsorption case especially for BC and AC adsorbents. Supplementary Fig. S4 and Fig. S5 show the results at MC and HC for the passive and active flow cases, respectively. Higher initial concentrations led to increased total mass of acetone removed, q_{total}, by factors of 1.4, 2.3, and 2.5, for CC, BC and AC, respectively.

The normalized removal rates for the active-flow experiments are shown in Fig. 8. Adsorption rates for fine CC (Fig. 8A) decreased slightly under the active flow conditions tested and did not change with increasing concentrations of acetone. This may be due to the flow velocity preventing the buildup of acetone on the CC surface. This hypothesis agrees with changes in the order of the rate model (n) between passive and active flow experiments, which decreased from ~1.2 to 0.9 after the addition of active flow.

Conversely, normalized adsorption rates for fine BC (Fig. 8B) and AC (Fig. 8C) increased significantly, with fine AC under active flow conditions achieving adsorption rates 50–100% greater in the first 2 h compared with passive flow experiments. Under active flow conditions, the order of the adsorption rate models for BC and AC increased by factors of 1.85 and 3.02, respectively.

4.6. Models for VOC removal in a nail salon

Mathematical models for VOC removal were constructed for the fine version of the 3 materials (CC, BC, and AC). Calculations were performed using different amounts of adsorbent material (10 kg, 50 kg, and 250 kg), under both passive and active flow conditions. Time-resolved VOC concentration data measured in a real nail salon during a single day were used as the input [5]. The volume of the salon used in the model was 1400 m^3. The total predicted VOC mass removal and effective ventilation rates (Q_{eff} and ACH_{eff}) for each case are shown in Table 2. Effective ventilation rates for fine AC under passive removal conditions ranged from 29.3 $m^3\ h^{-1}$ (0.02 ACH) to 222 $m^3\ h^{-1}$ (0.16 ACH) for 10 kg and 250 kg of AC, respectively. This was followed by fine BC and fine CC, which ranged from 18.2 $m^3\ h^{-1}$ to 182 $m^3\ h^{-1}$ and 16.7 $m^3\ h^{-1}$ to 179 $m^3\ h^{-1}$, respectively.

The use of jets was shown to remove significantly more VOCs for both fine AC and fine BC, where total mass removal values across cases increased by 31–94% and 17–39%, respectively. In the case of fine CC, VOC removal quantities decreased with the addition of jet flow by 43–65%.

Fig. 9 shows the results of the various simulations performed. Fig. 9A, C, and E show the predicted impact of CC, BC, and AC in the salon environment under passive flow conditions, respectively. Fig. 9B, D, and F show the impact of CC, BC, and AC under active flow conditions, respectively. Significant reductions in VOC concentrations are shown for all adsorbents at the 250 kg level; less significant reductions were produced with 50 kg and 10 kg of adsorbent. The largest removal was achieved with 250 Kg of fine AC and active flow (Fig. 9F), decreasing VOC concentrations to 0 mg m^{-3} in approximately 3 h and remaining there for the 8-h simulation period.

5. Discussion

VOC removal experiments with CC, BC, and AC showed that all 3 materials can adsorb VOCs under both passive and active flow conditions. Removal was also strongly linked to both ambient VOC concentrations and available adsorption sites, represented here as (1 - q(t)/q_{max}). Adsorbent particle size (e.g. fine or coarse) was shown to have relatively little effect on removal rates at LC. Results showed that material surface area and average pore size impacted the performance of the adsorbent material as VOC remover.

The use of SJA to provide local ventilation was shown to enhance the adsorption process for BC and AC in this study. Their use in actual indoor environments could be convenient and economical. For example, the minimum International Mechanical Code (IMC) ventilation rate for a 93 m^2 (1000 ft^2) salon is approximately 4.25 $m^3\ min^{-1}$ (150 CFM), which would require a 115 V blower operating at approximately 1 A (115 W). Comparatively, 115 W could power over 240 SJAs (consuming 475 mW each). As demonstrated by McQuillan [30], SJAs can impact

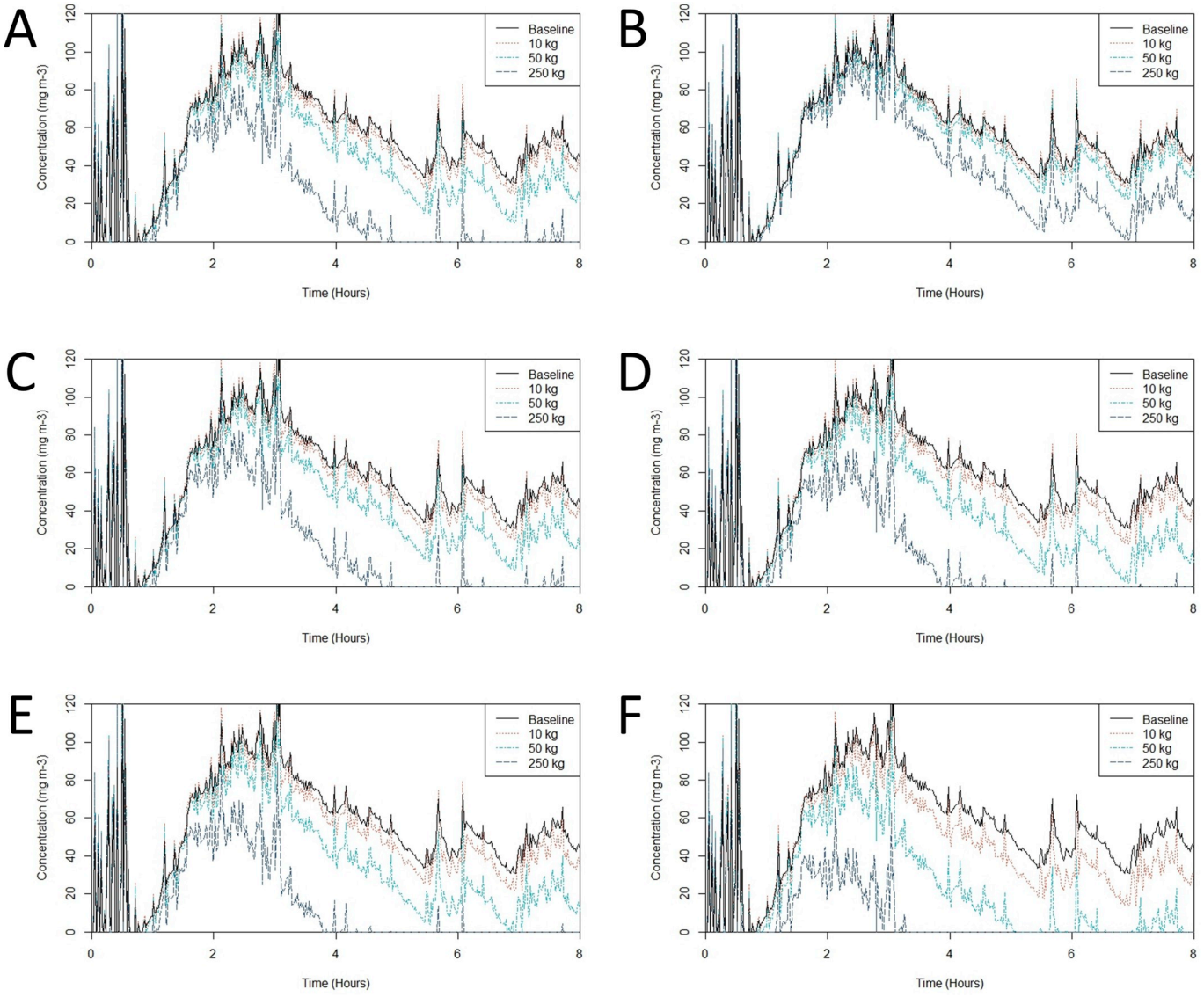

Fig. 9. Salon models for (A) CC passive flow, (B) CC active flow, (C) BC passive flow, (D) BC active flow, (E) AC passive flow, and (F) AC active flow.

flows from HVAC systems. In this study, SJAs were also shown to increase the removal of VOCs for BC and AC during the test period. Using synthetic jets to alter local flow conditions was especially advantageous for adsorbents with smaller average pore sizes as determined by BET and BJH analyses. This study did not attempt to optimize the placement of the SJA; therefore, it is possible that additional increases to the VOC removal rates could be achieved. Further, the placement of the SJA would be highly dependent on the configuration and the airflows of the room. Those experiments were beyond the scope of this study.

The VOC removal models showed that as little as 10 kg of AC could achieve a measurable reduction of VOCs in the nail salon environment, especially when active flow conditions are in effect. Additionally, effective ventilation rates calculated for all VOC removal models using 250 kg of adsorbent in passive flow conditions approached the minimum ventilation requirements set by the IMC for a 1400 m^3 nail salon (approximately 250 $m^3 h^{-1}$). When used in active flow conditions, 250 kg of fine AC was shown to achieve 0.21 ACH_{eff}, which is nearly 17% greater than the minimum ventilation rate published in the IMC for a nail salon of this volume [14]. Poor curve fits were obtained in some cases for CC and BC materials due to extreme non-linearity at the beginning of the experiments. This fast initial VOC removal may be due to preferential adsorbing onto fully available sites, a phenomenon previously documented by Ritchie [39]. Identifying the mechanism and obtaining better fits for this portion of the data would require more precise instrumentation and faster sampling rates than could be achieved in this study. This issue primarily affected data at the upper end of adsorption rates, leading to lower predicted adsorption values. The model presented here also did not account for the effect of concentration changes on $\dot{m}$ (Eq. (6)); which may be significant.

This study presents results that support the utilization of adsorbents in indoor environments with high VOC levels; however, further optimization of such systems is needed. For example, factors such as regeneration of the adsorbents and the location of these materials were not addressed here. Typically, adsorbents of this type are regenerated thermally at temperatures of less than 100 °C, which can be achieved using consumer-grade heating technology. The release of volatile compounds during regeneration processes presents a potential timing issue; however, regeneration cycles could be scheduled overnight, when building occupants are not present. Release of adsorbed VOCs during the night may have an added environmental benefit as well, since photolytic reactions that contribute to ozone and secondary organic aerosol (SOA) formation are unlikely to occur.

Although BC and CC were shown to remove VOCs from the air under both passive and active flow conditions, their removal capacities were

noticeably lower than commercial AC under all conditions tested in this study. When used under active flow conditions, BC achieved VOC removal comparable to commercial AC under passive flow conditions. This suggests that flow conditions should be considered during the optimization of adsorbent-based VOC removal systems for the indoor environment.

Although this study showed biochar to be an effective adsorbent for VOCs, it is also known to include residual pollutants as a result of the pyrolysis process under which it is generated. VOCs and polycyclic aromatic hydrocarbons (PAHs) have been found in biochars from a number of different feedstocks [41,42]. These compounds could potentially be released from the adsorbent materials into the indoor environment where they may affect the health of occupants [42]. Consequently, their use in air quality control applications will require additional research.

6. Conclusions

While biochar and coco coir used in this study were shown to remove VOCs from the ambient air, their removal capacities were both substantially lower than the commercially available activated carbon. This suggests that these alternative adsorbent materials may not be optimal for indoor VOC removal applications without some additional treatment to increase their adsorption capacity. The cost of such treatment should be considered when determining the advantages and disadvantages of these less common materials and removal systems. Reducing and capturing VOCs emitted in the indoor occupational environment is necessary to safeguard worker health, and may also help address urban ozone pollution and SOA formation. Results from this study are promising and suggest that indoor adsorbent sinks could play a role in future VOC mitigation efforts. In this study, directing ventilation to the adsorbent surface using a synthetic jet actuator led to increased VOC removal rates. Consequently, the combined use of adsorbent materials and localized active flows showed the best removal in these controlled experiments. Further exploration of these technologies should be conducted to address issues of material regeneration and implementation strategies, which were not covered in this study.

Funding

This study was supported by Grant Number T42OH009229-10 from CDC NIOSH Mountain and Plains Education and Research Center. The contents of this publication are solely the responsibility of the authors and do not necessarily represent the official views of the CDC NIOSH and MAP ERC. Additional support was provided by the CU Boulder Undergraduate Research Opportunities Program and the CU Engage Community-Based Research Fellowship Program.

Declaration of competing interest

None.

Appendix A. Supplementary data

Supplementary data to this article can be found online at https://doi.org/10.1016/j.buildenv.2019.106499.

References

[1] BLS, Employed Persons by Detailed Occupation, Sex, Race, and Hispanic or Latino Ethnicity, Labor Force Statistics from the Current Population Survey, Bureau of Labor Statistics, Washington, D.C, 2018. https://www.bls.gov/cps/cpsaat11.htm. (Accessed 24 July 2018).
[2] N.E. Klepeis, W.C. Nelson, W.R. Ott, J.P. Robinson, A.M. Tsang, P. Switzer, J. V. Behar, S.C. Hern, W.H. Engelmann, The National Human Activity Pattern Survey (NHAPS): a resource for assessing exposure to environmental pollutants, J. Expo. Sci. Environ. Epidemiol. 11 (2001) 231–252.
[3] G.A. Ayoko, H. Wang, Indoor air pollution, 2nd edition: volatile organic compounds in indoor environments, Hdb Env. Chem. 64 (2018) 69–108.
[4] K. Badjagbo, S. Loranger, S. Moore, R. Tardif, S. Suave, BTEX exposures among automobile mechanics and painters and their associated health risks, Hum. Ecol. Risk Assess. 16 (2) (2010) 301–316.
[5] A. Lamplugh, M. Harries, F. Xiang, J. Trinh, A. Hecobian, L.D. Montoya, Occupational exposure to volatile organic compounds and health risks in Colorado nail salons, Environ. Pollut. 249 (2019) 518–526.
[6] V.M. Alaves, D.K. Sleeth, M.S. Thiese, R.R. Larson, Characterization of indoor air contaminants in a randomly selected set of commercial nail salons in Salt Lake County, Utah, USA, Int. J. Environ. Health Res. 23 (2013) 419–433.
[7] T. Quach, R. Gunier, A. Tran, J. Von Behren, P.A. Doan-Billings, K.D. Nguyen, L. Okahara, B.Y. Lui, M. Nguyen, J. Huynh, P. Reynolds, Characterizing workplace exposures in Vietnamese women working in California nail salons, Am. J. Public Health 101 (Suppl 1) (2011) S271–S276.
[8] E. Huzar, A. Wodnicka, M. Dzieciol, Analysis of volatile compounds in nail polish removers as a criterion of health hazard determination and commodity evaluation, Ecol. Chem. Eng. A. 18 (7) (2011) 991–998.
[9] L. Zhong, S. Batterman, C.W. Milando, VOC sources and exposures in nail salons: a pilot study in Michigan, USA, Int. Arch. Occup. Environ. Health 92 (1) (2019) 141–153.
[10] U.S. EPA, Protecting the Health of Nail Salon Workers, U.S. Environmental Protection Agency, Washington, D.C, 2007. EPA/744/F-07/001, https://www.epa.gov/sites/production/files/2015-05/documents/nailsalonguide.pdf. (Accessed 2 December 2017).
[11] E.M. John, D.A. Savitz, C.M. Shy, Spontaneous abortions among cosmetologists, Epidemiology 5 (1994) 147–155.
[12] J.A. Swenberg, B.C. Moeller, K. Lu, J.E. Rager, R.C. Fry, T.B. Starr, Formaldehyde carcinogenicity research: 30 Years and counting for mode of action, epidemiology, and cancer risk assessment, Toxicol. Pathol. 41 (2013) 181–189.
[13] C. Roelofs, T. Do, Exposure assessment in nail salons: an indoor air approach, Int. Sch. Res. Notices 2012 (2012) 7.
[14] L.J. Goldin, L. Ansher, A. Berlin, J. Cheng, D. Kanopkin, A. Khazan, M. Kisivuli, M. Lortie, E.B. Peterson, L. Pohl, S. Porter, V. Zeng, T. Skogstrom, M.A. Fragala, T. A. Myatt, J.H. Stewart, J.G. Allen, Indoor air quality survey of nail salons in Boston, J. Immigr. Minority Health 16 (2014) 508–514.
[15] ICC, International Mechanical Code, International Code Council, Inc., Washington, D.C, 2015, ISBN 978-1-60983-479-1.
[16] ELI, Indoor Air Quality in Nail Salons: Developments in State Policy, Environmental Law Institute, Washington, D.C, 2017. https://www.eli.org/buildings/indoor-air-quality-nail-salons. (Accessed 21 April 2019).
[17] B. Pavilonis, C. Roelofs, C. Blair, Assessing indoor air quality in New York City nail salons, J. Occup. Environ. Hyg. 15 (5) (2018) 422–429.
[18] X. Zhang, B. Gao, A.E. Creamer, C. Cao, Y. Li, Adsorption of VOCs onto engineered carbon materials: a review, J. Hazard Mater. 338 (2017) 102–123.
[19] I.K. Shah, P. Pre, B.J. Alappat, Effect of thermal regeneration of spent activated carbon on volatile organic compound adsorption performances, J. Taiwain Inst. Chem. Eng. 45 (4) (2014) 1733–1738.
[20] R. Meininghaus, L. Gunnarsen, H.N. Knudsen, Diffusion and sorption of volatile organic compounds in building materials - impact on indoor air quality, Environ. Sci. Technol. 34 (15) (2000) 3101–3108.
[21] K.-C. Huang, Y.-S. Tsay, F.-M. Lin, C.-C. Lee, J.-W. Chang, Efficiency and performance tests of the sorptive building materials that reduce indoor formaldehyde concentrations, PLoS One 14 (1) (2019), e0210416, https://doi.org/10.1371/journal.pone.0210416. (Accessed 3 March 2019).
[22] M.S. Zuraimi, R.J. Magee, D.Y. Won, G. Nong, C.D. Arsenault, W. Yang, S. So, G. Nilsson, L. Abebe, C. Alliston, Performance of sorption and photocatalytic oxidation-based indoor passive panel technologies, Build. Environ. 135 (2018) 85–93.
[23] M.T. Moreira, I. Noya, G. Feijoo, The prospective use of biochar as adsorption matrix - a review from a lifecycle perspective, Bioresour. Technol. 246 (2017) 135–141.
[24] X. Zhang, B. Gao, Y. Zheng, X. Hu, A.E. Creamer, M.D. Annable, Y. Li, Biochar for volatile organic compound (VOC) removal: sorption performance and governing mechanisms, Bioresour. Technol. 245 (2017) 606–614.
[25] M.-S. Li, S.C. Wu, Y.-H. Peng, Y.-H. Shih, Adsorption of volatile organic vapors by activated carbon derived from rice husk under various humidity conditions and its statistical evaluation by linear solvation energy relationships, Separ. Purif. Technol. 170 (2016) 102–108.
[26] R. Malik, S. Dahiya, S. Iata, An experimental and quantum chemical study of removal of utmostly quantified heavy metals in wastewater using coconut husk: a novel approach to mechanism, Int. J. Biol. Macromol. 98 (2017) 139–149.
[27] S.B. Gautam, M.S. Alam, S. Kamsonlian, Adsorptive removal of as(III) from aqueous solution by raw coconut husk and iron impregnated coconut husk: kinetics and equilibrium analyses, Int. J. Chem. React. Eng. 15 (2) (2016) 2194–5748.
[28] Alexander, D., Ellerby, R., Hernandez, A., Wu, F., Amarasiriwardena, D., Investigation of simultaneous adsorption properties of Cd, Cu, Pb and Zn by pristine rice husks using ICP-AES and LA-ICP-MS analysis. Michrochem. J. 135, 129–139.
[29] C.P. Hoang, K.A. Kinney, R.L. Corsi, Ozone removal by green building materials, Build. Environ. 44 (8) (2009) 1627–1633.
[30] B. McQuillan, J. Hertzberg, L.D. Montoya, Flow visualization study of synthetic flow control in the indoor environment, Build. Environ. 73 (2014) 239–248.
[31] L.D. Montoya, D.C. Mauney, W.V. Srubar III, Investigation of efficient air pollutant removal using active flow control, Build. Environ. 122 (2017) 134–144.

[32] L.D. Montoya, J.L. Jackson, M. Amitay, Control of aerosol dispersion and removal in a room using synthetic jet actuators, Build. Environ. 45 (2010) 165–175.
[33] Z.-Y. Li, Y. Xu, L.-H. Feng, J.-J. Wang, Synthetic jet vortex rings impinging onto a porous wall: Reynolds number effect, Int. J. Heat Mass Transf. 137 (2019) 951–967.
[34] M. Abarr, D. Mauney, J. Hertzberg, L.D. Montoya, Characterization of a commercial synthetic jet actuator for air quality applications, J. Fluids Eng. 139 (7) (2017) 7.
[35] Y. Ataka, S. Kato, S. Murakami, Q. Zhu, K. Ito, T. Yokota, Study of effect of adsorptive building material on formaldehyde concentrations: development of measuring methods and modeling of adsorption phenomena, Indoor Air 14 (Suppl. 8) (2004) 51–64.
[36] J. Rouquerol, D. Avnir, C.W. Fairbridge, D.H. Everett, J.M. Haynes, N. Pernicone, J. D.F. Ramsay, K.S.W. Sing, K.K. Unger, Recommendations for the characterization of porous solids, Pure Appl. Chem. 66 (8) (1994) 1739–1758.
[37] C.W. Cheung, J.F. Porter, G. McKay, Elovich equation and modified second-order equation for sorption of cadmium ions onto bone char, J. Chem. Technol. Biotechnol. 75 (2000) 963–970.
[38] H. Huang, F. Haghighat, P. Blondeau, Volatile Organic Compound (VOC) adsorption on material: influence of gas phase concentration, relative humidity, and VOC type, Indoor Air 16 (2006) 236–247.
[39] A.G. Ritchie, Alternative to the elovitch equation for the kinetics of adsorption of gases on solids, J. Chem. Soc. Faraday Trans. I 73 (1977) 1650–1653.
[40] Y. Liu, L. Shen, A general rate law equation for bioadsorption, Biochem. Eng. J. 38 (2008) 390–394.
[41] T. Dutta, E. Kwon, S.S. Bhattacharya, B.H. Jeon, A. Deep, M. Uchimiya, K.-H. Kim, Polycyclic aromatic hydrocarbons and volatile organic compounds in biochar and biochar-amended soil: a review, Glob. Change Biol. Bioenergy. 9 (2017) 990–1004.
[42] W. Buss, O. Mašek, High-VOC biochar – effectiveness of post-treatment measures and potential health risks related to handling and storage, Environ. Sci. Pollut. Res. 23 (2016) 19580–19589.

Supplementary Information - Tables and Figures

Table S1. List of nail care products used in this study.

Identifier	Product Class	Volatile Ingredients (from SDS)	Volatile Content (from SDS)
NP-1	Nail Polish	n-butyl acetate, ethyl acetate, isopropyl alcohol, propyl acetate, camphor	50.2 – 100%*
NP-2	Nail Polish	n-butyl acetate, ethyl acetate, isopropyl alcohol, propyl acetate, n-butyl alcohol, ethanol, heptane, camphor	55 – 100%*
NP-3	Nail Polish	n-butyl acetate, ethyl acetate, isopropyl alcohol, n-butyl alcohol	50 – 62%
PR-1	Nail Polish Remover	methyl acetate, dimethyl glutarate, SD Alcohol 40, methyl alcohol	16 – 45%
PR-2	Nail Polish Remover	Acetone	Not Provided

*Volatile content presented is the sum of all volatile ingredients listed for each product in the SDS. Since individual compound values were provided as a range, the sum total in some cases exceeded 100%.

Table S2. Fitting values for model based on Eq. 9 using PR-2 as the model VOC

Passive Flow		**a**	**n**	**R^2**	**Spearman ρ**
Fine CC	LC	3.167E-5	1.176E+0	0.718	0.856
	MC	3.167E-5	1.176E+0	0.780	0.925
	HC	3.167E-5	1.176E+0	0.949	0.943
Fine BC	LC	3.098E-5	4.447E-1	0.680	0.935
	MC	3.098E-5	4.447E-1	0.678	0.920
	HC	3.098E-5	4.447E-1	0.862	0.971
Fine AC	LC	5.124E-5	3.261E-1	0.874	0.941
	MC	5.124E-5	3.261E-1	0.863	0.956
	HC	5.124E-5	3.261E-1	0.969	0.990
Active Flow		**a**	**b**	**R^2**	**Spearman**
Fine CC	LC	9.852E-6	9.091E-1	0.843	0.839
	MC	9.852E-6	9.091E-1	0.740	0.823
	HC	9.852E-6	9.091E-1	0.400	0.446
Fine BC	LC	4.635E-5	8.231E-1	0.869	0.917
	MC	4.635E-5	8.231E-1	0.825	0.968
	HC	4.635E-5	8.231E-1	0.874	0.983
Fine AC	LC	1.234E-4	9.862E-1	0.966	0.969
	MC	1.234E-4	9.862E-1	0.982	0.985
	HC	1.234E-4	9.862E-1	0.975	0.989

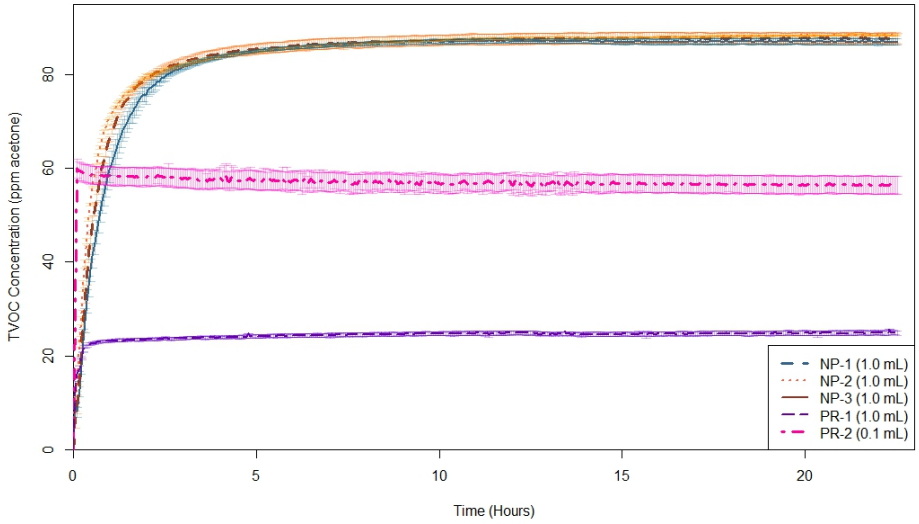

Fig. S1. Baseline TVOC emission profiles from 5 nail products over 22.5 h with standard error bars. Emissions from the 3 nail polishes (NP) were fairly similar but considerably different from the nail polish removers (PR). The nail polish removers were also fairly different from each other. TVOC emissions are reported in terms of equivalent ppm of acetone. NP reached equilibrium in about 5 h compared to PR, which reached equilibrium in < 1 h. This difference likely reflects the fact that NP were composed of more volatile compounds methyl acetate (boiling point 56.9 °C) and acetone (boiling point 56.1 °C). In contrast, the primary ingredient in all NP was ethyl acetate (boiling point 77.1°C).

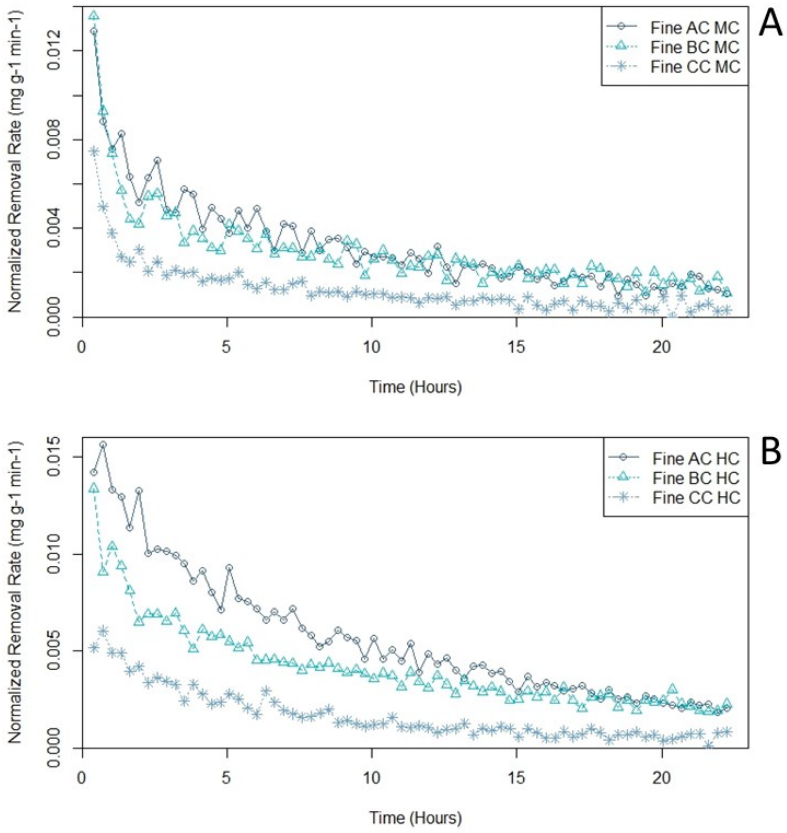

Fig. S2. Passive VOC Removal rates of fine AC, BC, and CC at (A) MC and (B) HC across 22.5 h

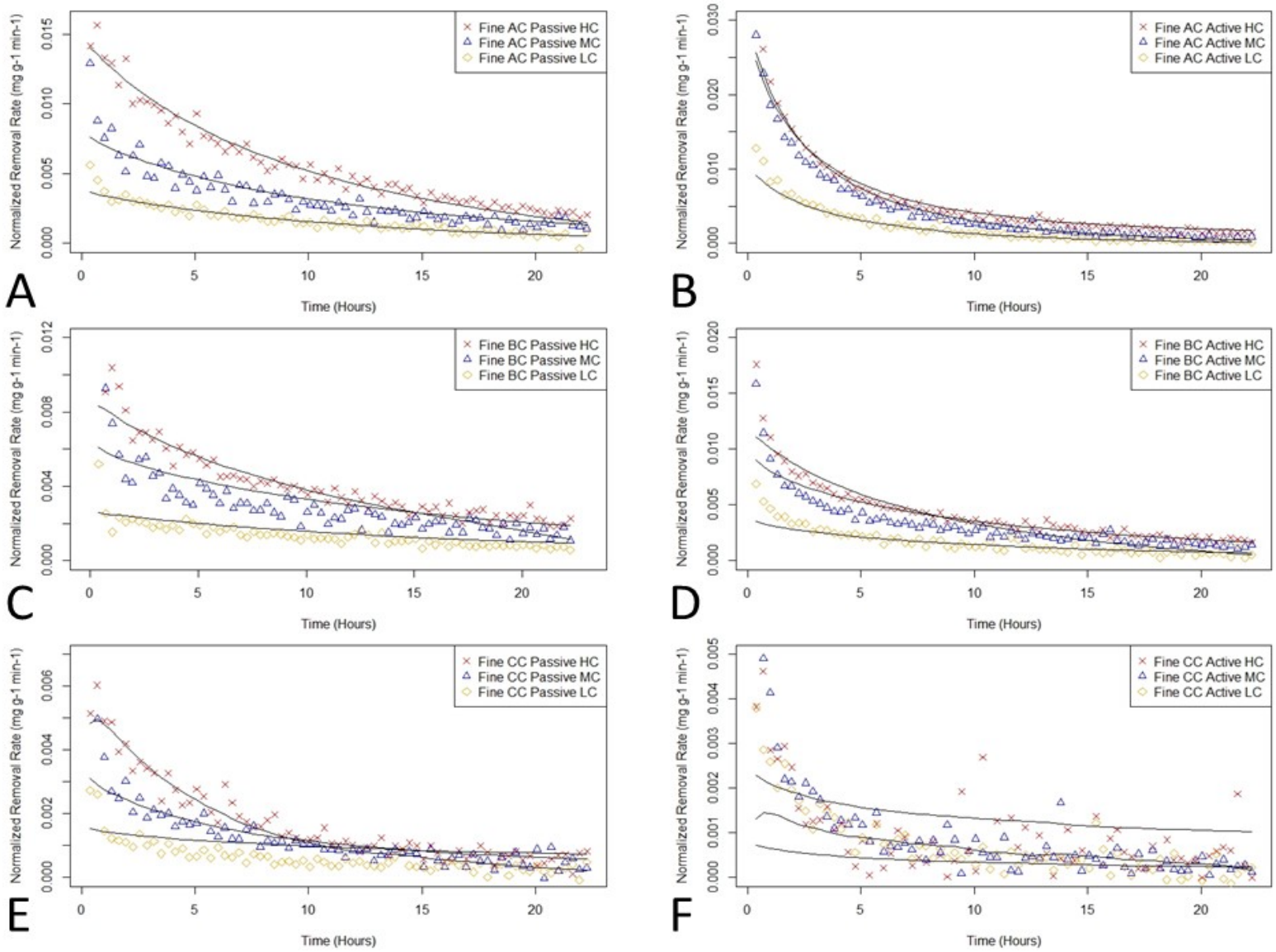

Fig. S3. Fitted VOC removal rate data of fine grain materials: (A) AC Passive Flow, (B) AC Active Flow, (C) BC Passive Flow, (D) BC Active Flow, (E) CC Passive Flow, and (F) CC Active Flow

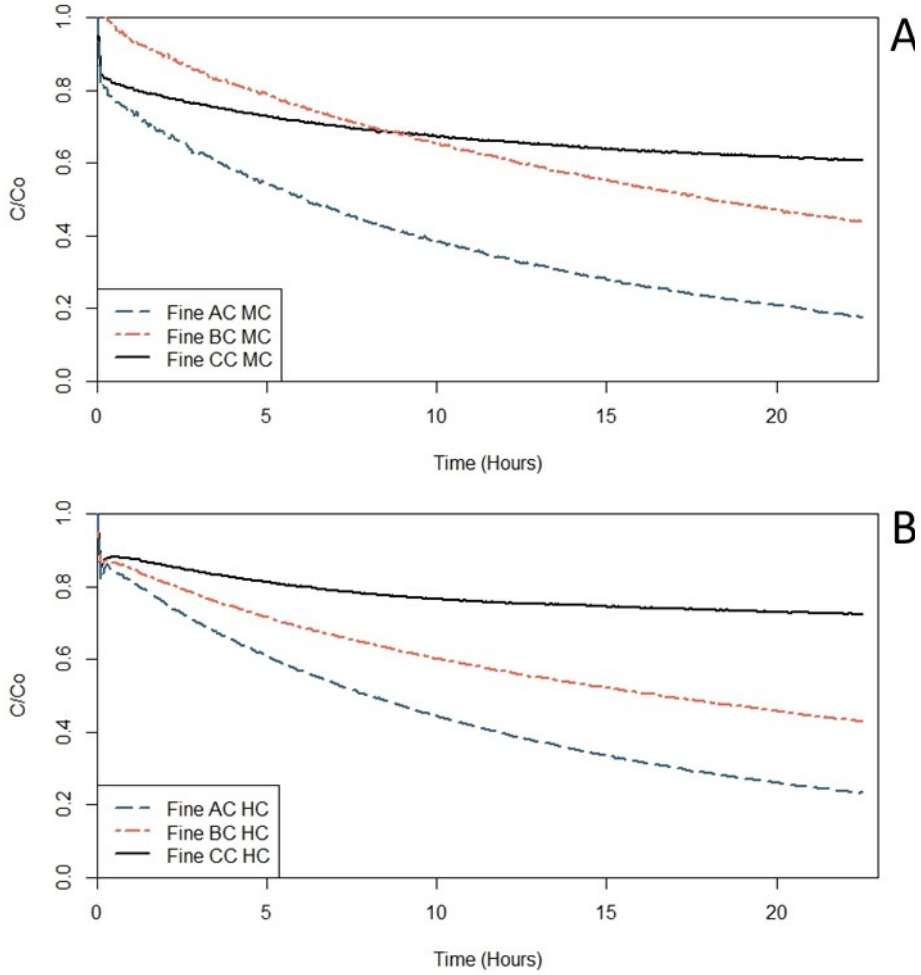

Fig. S4. Passive VOC removal of fine AC, BC, and CC at (A) MC and (B) HC during 22.5 h

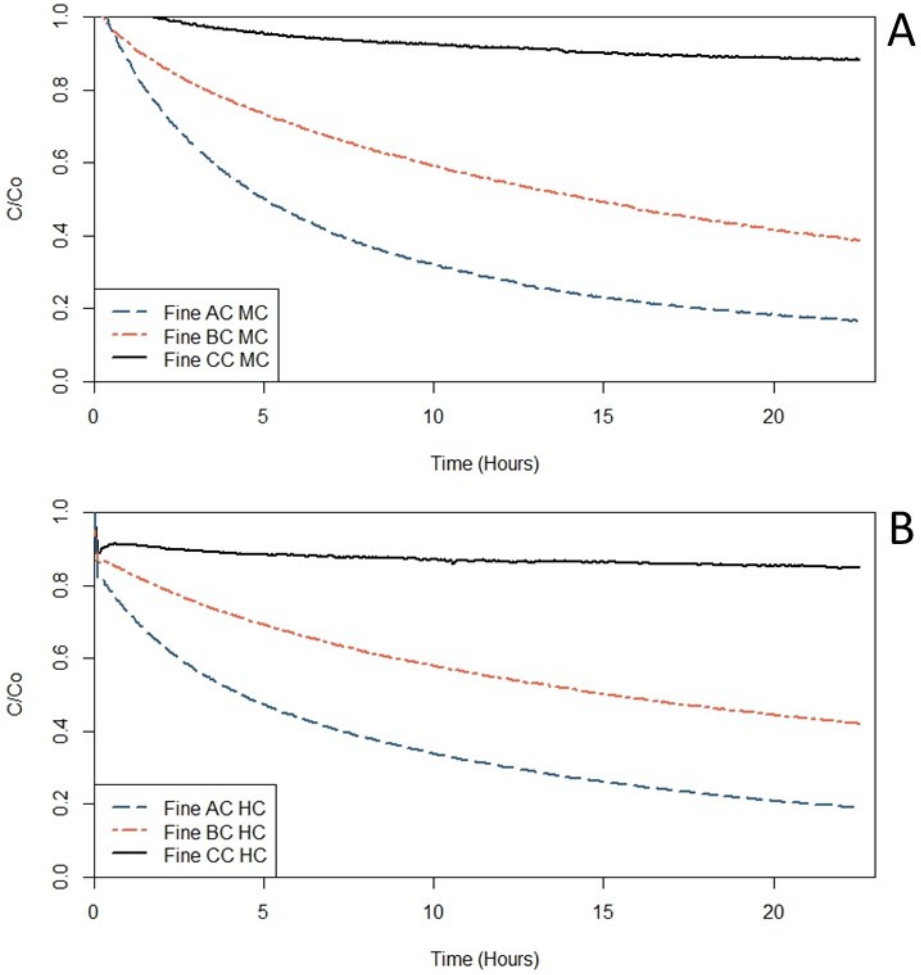

Fig. S5. Active VOC removal of fine AC, BC, and CC at (A) MC and (B) HC during 22.5 h

PRODUCT DATASHEET

Supplementary Information
Appendix A

SynJet® LED Cooler R87-60

SynJet cooling technology provides the most reliable thermal management solution available. This LED cooler has been developed by Nuventix for cooling downlight and spotlight modules and arrays.

- Cools up to 45 W[4]
- Reliable 100K Hours Lifetime
- Energy Efficient
- 5 Yr Warranty
- Small Form Factor
- Quiet Acoustics

Specifications[1]

Thermal & Acoustic

SynJet Setting[2]	Θs-a[3] Al	TDP[4] (W) ΔT = 30° / 40°C	SPL (dBA)[5]	Wire Connections	
Mid Performance	0.70	43 / 57	25	Red to +VDC Black & Blue to Ground	
Standard Performance	0.78	38 / 51	22	Red to +VDC Black only to Ground	
Silent Performance	0.91	33 / 44	19	Red to +VDC Black & Purple to Ground	
PWM at 100% duty cycle	0.66	45 / 61	27	Red to +VDC Black only to Ground Blue to PWM Signal	
Heatsink Only	2.02	15	N/A	N/A	N/A

Electrical

SynJet Setting[2]	Voltage (VDC) +/- 10%	Current (mA)[6]			Pavg (mW)	Voltage (VDC) +/- 10%	Current (mA)[6]			Pavg (mW)
		Imin	Iavg	Ipeak			Imin	Iavg	Ipeak	
Mid	5	20	150	300	750	12	10	67	134	800
Standard			95	190	475			50	100	600
Silent			65	130	325			40	80	480
PWM at 100% duty cycle			160	320	800			82	164	980

Environmental

All Settings	Min	Max	Units	Conditions
Operating Temperature	-40	70	°C	Air temperature surrounding cooler
Storage Temperature	-50	75	°C	Air temperature surrounding cooler
Storage Altitude		15K	m	Above sea level
Operating Relative Humidity	5	95	%	Non-condensing
Weight		335	g	SynJet with Al heat sink
Reliability		100K	hrs	L10 @ 60°C
Regulatory Compliance				RoHS, UL, FCC Part 15 Class B, CE

[1] All values are typical at 25ºC unless otherwise stated.
[2] The Level Select model should be used for discrete performance settings. Follow the instructions in the Product Design Guide for adjusting settings.
[3] Thermal resistance values are given as reference only and are measured in free air without airflow obstructions. Thermal resistance is measured from the bottom middle of the heat sink to ambient air measured at the inlet to the SynJet, with a heat source at least 4.1cm^2 using the 60 W reference heat sink. Actual thermal performance may vary by application and final product design should be tested to assure proper thermal performance.
[4] Thermal Design Power is based on a 30ºC or 40ºC temperature rise of heat sink mounting surface above ambient temperature around cooler.
[5] Sound Pressure Level is measured at 1 meter distance per ISO 7779.
[6] The SynJet has a time varying current. The current waveform is sinusoidal and the average current (Iavg) is used to calculate the average power consumption (Pavg) at nominal input voltage (VDC). See the Electrical section in the Product Design Guide for a detailed explanation.

Mechanical - SynJet Cooling Solution shown with Configurable heat sink

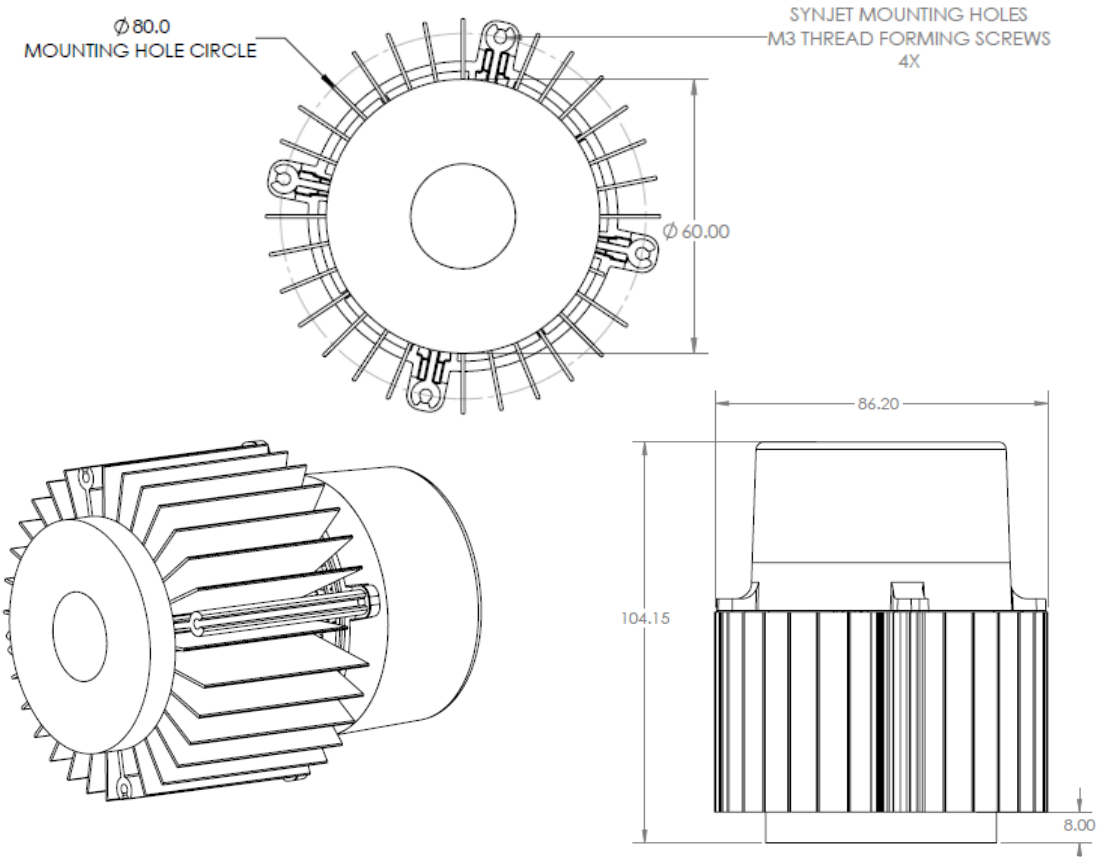

All dimensions are nominal and in mm unless otherwise stated. See product drawings for more detail.

SynJet Wire Harness

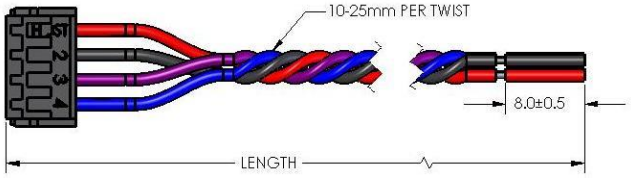

Connector Pinout

Pin	Wire Color	Symbol	Description
1	Red	+VDC	5 V or 12 V depending on model
2	Black	GND	Ground
3	Purple	CTRL2	Input for Level Select model Status signal for PWM model
4	Blue	CTRL1	Input for Level Select model PWM input for PWM model

IMPORTANT: SynJets should be completely wired to the power supply before the power supply is energized. The power supply should be turned off before the SynJet Cooler is disconnected. SynJet Coolers are not designed for “hot swap” or “hot plug” applications.

Part Numbers

Part Number	Description	Notes
NX201100	SynJet, ZFlow 87, PWM, 5V, Black	Use with PWM input to control performance setting
NX201101	SynJet, ZFlow 87, Level Select, 5V, Black	Configurable to discrete performance settings
NX201102	SynJet, ZFlow 87, PWM, 12V, Black	Use with PWM input to control performance setting
NX201103	SynJet, ZFlow 87, Level Select, 12V, Black	Configurable to discrete performance settings
NX301105	Heatsink, R87-60, Xicato XSM M3, Vossloh Schwabe Luga Shop, Black	Contact sales for other heatsink options
NX301106	Heatsink, R87-60, Citizen CLL030, CLL050, Ledil, Black	Contact sales for other heatsink options
NX301107	Heatsink, R87-60, Osram Soleriq, Ledil, Sharp Megazenigata, Molex, Black	Contact sales for other heatsink options
NX301108	Heatsink, R87-60, Philips Luxeon K, Black	Contact sales for other heatsink options
NX301114	Heatsink, R87-60, Config, Black	Contact sales for other heatsink options
NX301115	Heatsink, R87-60, Bridgelux Vero 13/18, Black	Contact sales for other heatsink options
NX301117	Heatsink, R87-60, Bridgelux Vero 29, RS, Black	Contact sales for other heatsink options
WALLS-C4150-001	Wire Harness, 4-Wire, 150 mm Length	Contact sales for other wire harness options
WALLS-C4600-001	Wire Harness, 4-Wire, 600 mm Length	Contact sales for other wire harness options